

Hard Magnets Based on Layered Cobalt Hydroxide: The Importance of Dipolar Interaction for Long-Range Magnetic Ordering[†]

Mohamedally Kurmoo*

*Institut de Physique et Chimie des Matériaux de Strasbourg, 23 Rue du Loess,
67037 Strasbourg Cedex, France*

Received July 9, 1999

The synthesis of $\text{Co}_5(\text{OH})_8(\text{C}_7\text{H}_{15}\text{CO}_2)_2 \cdot 4\text{H}_2\text{O}$, $\text{Co}_5(\text{OH})_8(\text{O}_2\text{CC}_6\text{H}_{12}\text{CO}_2) \cdot 5\text{H}_2\text{O}$, $\text{Co}_5(\text{OH})_8(\text{C}_{12}\text{H}_{25}\text{SO}_4)_2 \cdot (3\text{H}_2\text{O} \cdot 2\text{NH}_3)$, and $\text{Co}_5(\text{OH})_8(\text{C}_2\text{N}_3)_2 \cdot 6\text{H}_2\text{O}$, their characterization by electron microscopy, XRD, TGA, IR, UV–vis, and XANES, and their magnetic properties are reported. They belong to a family of layered compounds having a triangular magnetic lattice. The basal spacing is 22.8, 16.2, 25.0, and 11.5 Å for the carboxylate, dicarboxylate, sulfate, and cyanide, respectively. From the powder X-ray and crystal electron diffraction data, the compounds are inferred to adopt the structure of the monoclinic form of $\text{Zn}_5(\text{OH})_8\text{X}_2 \cdot \text{solvent}$. XANES confirms that only divalent cobalt is present in the compounds and visible absorption spectra display bands originating from both octahedral and tetrahedral coordinated Co^{II} and none from Co^{III} . The magnetic data show that all the compounds behave as two sublattice ferrimagnets which are characterized by a minimum in the temperature dependence of the moments and long-range ordering observed by spontaneous magnetization in small dc applied field, out-of-phase components in the ac magnetization and hysteresis loop. The saturation magnetization, approaching $3 \mu_{\text{B}}$ at 2 K in field of 5 T, is in good agreement with the proposed structure consisting of three Co^{II} in octahedral coordination in one sublattice and two Co^{II} in tetrahedral coordination for the other. The Curie temperature attains 58 K and coercive field approaches 12 000 Oe at 2 K. The long-range ordering is driven by dipolar interaction between layers which have large effective moment resulting from short-range intralayer interactions. Interestingly, the Curie temperatures are independent of the chemical and physical nature of the anions, as expected for the proposed dipolar mechanism. The large coercive fields result from the synergy of crystalline shape and single ion anisotropies and to the alignment of the moments perpendicular to the layers.

Introduction

One area of solid-state chemistry that has shown remarkable growth over the last 10 years is that involving the synthesis and characterization of metal–organic and organic magnetic materials.¹ The main aim being to establish long-range magnetic ordering for which different approaches have been developed; much of the effort is devoted to aligning the moment carriers, i.e., the magnetic orbital, in some desired fashion in the crystalline solids. Although most of the compounds showing long-range magnetic ordering are serendipitously obtained, there is increasing success in the development of multitopic ligands acting as connectors that are able to organize magnetic centers.² The remarkable increase in the number of metal–organic magnetic materials and the success in the design of

connectors have fueled an enormous amount of basic and applied research.

One key element for the observation of magnetic ordering is the relative alignment of the magnetic orbital of near neighbors within the lattice.^{1a} The second element is the nature of the bridging unit between the magnetic centers as it defines the magnitude of the exchange interaction³ and consequently, the transition temperatures of the magnetic ordering. For example, we can compare the Curie temperatures (T_{C}) of 3D lattices where all near neighbors are connected through equivalent bridging connectors. For pure metals (no bridging unit), T_{C} is greater than 1000 K,⁴ for those with

* E-mail: kurmoo@friss.u-strasbg.fr.

[†] Non-SI units are employed: $1 \text{ T} = 10\,000 \text{ Oe} \approx 7.96 \times 10^5 \text{ A m}^{-1}$; $1 \mu_{\text{B}} \approx 9.3 \times 10^{-24} \text{ J T}^{-1}$.

(1) (a) Kahn, O.; Journaux, Y. In *Inorganic Materials*; Bruce, D., O'Hare, D., Eds.; John Wiley: New York, 1992. (b) Kahn, O. *Adv. Inorg. Chem.* **1995**, *43*, 179. (c) Kahn, O., Ed. *Magnetism: A supramolecular function*; NATO ASI series C484; Kluwer Academic Publishers: Dordrecht, 1996. (d) *Mol. Cryst. Liq. Cryst.* **1993**, *232*; **1995**, *273*; **1997**, *305*; **1999**, *334*. (e) Veciana, J.; Rovira, C.; Amabilino, D. B., Eds. *Supramolecular engineering of synthetic metallic materials*; NATO ASI C518; Kluwer Academic Publishers: Netherlands, 1998.

(2) (a) Broderick, W. E.; Thompson, J. A.; Day, E. P.; Hoffman, B. M. *Science* **1990**, *249*, 410. (b) Stumpf, H. O.; Ouahab, L.; Pei, Y.; Grandjean, D.; Khan, O. *Science* **1993**, *261*, 447. (c) Heintz, R. A.; Zhao, H.; Ouyang, X.; Grandinetti, G.; Cowen, J.; Dunbar, K. R. *Inorg. Chem.* **1999**, *38*, 144. (d) Zhao, H.; Heintz, R. A.; Ouyang, X.; Dunbar, K. R.; Campana, C. F.; Rogers, R. D. *Chem. Mater.* **1999**, *11*, 736. (e) Gutschke, S. O. H.; Price, D. J.; Powell, A. K.; Wood, P. T. *Angew. Chem., Int. Ed.* **1999**, *38*, 1088. (f) Ohba, M.; Fukita, N.; Okawa, H. *J. Am. Chem. Soc.* **1997**, *119*, 1011.

(3) (a) Goodenough, J. B. *Magnetism and the Chemical Bond*; John Wiley and Sons: New York, 1963. (b) De Jongh, L. J.; Miedema, A. R. *Adv. Phys.* **1974**, *23*, 1.

(4) Conolly, T. F.; Copenhaver, E. D. *Bibliography of magnetic materials and tabulation of magnetic transition temperatures, Solid State Physics Literature Guides*; IPI/Plenum: New York, 1972; Vol. 5.

one atom connector (e.g., oxides)⁴ T_C can reach up to 800 K and for those with two atoms connectors (e.g., cyanides of the Prussian blue family)⁵ T_C is nearly 400 K. We⁶ and others^{7,8} have recently prepared and characterized the first series of transition metals complexes, based on the dicyanamide ligand ($N\equiv C-N-C\equiv N$), having a three-atom bridge, $\cdots N-C\equiv N\cdots$, between the centers; the highest T_C observed is 21 K. However, it is clear from this comparison that increasing the size of the bridging units will not result in higher Curie temperatures. It is also evident from data available in the literature that bridging units with π -bonding are more efficient than those with only σ -bonding.

In the three-dimensional systems mentioned above, the magnetic exchange pathways are isotropic and equivalent or nearly equivalent. In the layered magnetic systems based on the oxalates,⁹ perovskites,¹⁰ insertion compounds of MPS₃,¹¹ metal sulfides,¹² and manganites,¹³ high Curie temperatures have been observed for moments separated by several atoms, or in some cases where there exist no chemical connection between the layers. Therefore, we have recently embarked on the idea of introducing controllable anisotropy in the exchange interactions by systematically tuning the interlayer spacing of layered compounds consisting of moment carriers separated by only one atom within the layer. It was hoped that the critical temperature may be tuned continuously and that it may be possible to relate T_C to the statistical average of the number of intervening atoms between the moments.¹⁴ However, this approach has resulted in some unexpected and unusual observations: (a) of ferrimagnets with Curie

temperatures of nearly 60 K for interlayer spacing of as much as 25 Å and coercive field as high as 19 000 Oe at 2 K^{14a} and (b) a metamagnet displaying a hysteresis loop with a coercive field in excess of 50 000 Oe.^{14b} Consequently, we have developed a synthetic route to prepare and have characterized a series of magnetic layered compounds based on the rigid brucite-like metal hydroxide triangular lattice (M–M distance of ~ 3 Å)¹⁵ where the interlayer separation can be tuned from 9 to 29 Å by changing the shape and size of the anion, for example, the alkyl chain length of the anion separating the layers. Several anions containing carboxylate, dicarboxylate, sulfate, sulfonate, and cyanide end groups have been employed. We have also varied the moment carriers from $S = 1/2$ (Cu) to $S = 1$ (Ni) to $S = 3/2$ (Co)^{14a} and between 1 and $3/2$ by synthesizing Ni–Co solid-solutions. The copper compounds exhibit short-range antiferromagnetic interactions. The nickel compounds are ferromagnetic with Curie temperatures reaching 25 K and coercive fields less than 1000 Oe. Two families of cobalt compounds have been synthesized.^{14b} The first family, $Co_5(OH)_8X_2 \cdot \text{solvent}$, behaves as ferrimagnet with Curie temperature attaining 60 K and coercive fields of nearly 20 000 Oe and the second family behaves as metamagnet with an unprecedented magnetic hardness resulting in a coercive field in excess of 50 000 Oe in the case of $Co_4(OH)_2(\text{terephthalate})_3 \cdot (NH_3)_{1.5}(H_2O)_{2.5}$.^{14b} Here, we report the results of four compounds belonging to the ferrimagnet set with a variety of anions and show that the Curie temperature is not influenced by either the distance between the layers or the chemical and physical nature of the spacers, and whether the layers are covalently bonded or not.

From a magnetic point of view, these compounds are of additional interest for three main reasons. First, the triangular arrangement of the spin carriers is of theoretical importance with regard to frustration¹⁶ and to the question of long-range order in two dimension.¹⁷ Second, the possibility of introducing guest molecules in the galleries between the layers provide a way to tune one magnetic exchange independently while keeping those within the layer unaltered and allows one to introduce other spin carriers, optically active molecules and electron or hole carriers for creating structures with combined properties.¹⁸ Third, when the layers are well-separated one can consider them as multiple stacks of single layer magnets.¹⁹ If the moments have perpendicular alignment, they can be of great commercial value for high-density magnetic recording materials; an area of research which is very active.²⁰

(5) (a) Gadet, V.; Mallah, T.; Castro, I.; Verdaguer, M. *J. Am. Chem. Soc.* **1992**, *114*, 9213. (b) Mallah, T.; Thiebaut, S.; Verdaguer, M.; Veillet, P. *Science* **1993**, *262*, 1554. (c) Entley, W. R.; Girolami, G. S. *Science* **1995**, *268*, 397. (d) Babel, D. *Inorg. Chem.* **1986**, *5*, 285. (e) Vernier, N.; Bellessa, G.; Mallah, T.; Verdaguer, M. *Phys. Rev. B* **1997**, *56*, 75. (f) Sato, O.; Iyoda, T.; Fujishima, A.; Hashimoto, K. *Science* **1996**, *271*, 49. (g) Verdaguer, M. Personal communication.

(6) (a) Kurmoo, M.; Kepert, C. J. *New J. Chem.* **1998**, *22*, 1515. (b) Kurmoo, M.; Kepert, C. J. *Mol. Cryst. Liq. Cryst.* **1999**, *334*, 693.

(7) (a) Batten, S. R.; Jensen, P.; Moubaraki, B.; Murray, K. S.; Robson, R. *Chem. Commun.* **1998**, 439. (b) Jensen, P.; Batten, S. R.; Fallon, G. D.; Moubaraki, B.; Murray, K. S.; Price, D. J. *Chem. Commun.* **1999**, 177.

(8) Manson, J. L.; Kmety, C.; Huang, Q.; Lynn, J. W.; Bende, G.; Pagola, S.; Stephens, P. W.; Epstein, A. J.; Miller, J. S. *Chem. Mater.* **1998**, *10*, 2552.

(9) (a) Tamaki, H.; Zhong, Z. J.; Matsumoto, N.; Kida, S.; Koikawa, M.; Achiwa, N.; Hashimoto, Y.; Ookawa, H. *J. Am. Chem. Soc.* **1992**, *114*, 6974. (b) Decurtins, S.; Schmalke, H. W.; Schneuwly, P.; Ensling, J.; Gülich, P. *J. Am. Chem. Soc.* **1994**, *116*, 9521. (c) Mathoniere, C.; Carling, S. G.; Yusheng, D.; Day, P. *J. Chem. Soc., Chem. Commun.* **1994**, 1551. (d) Nuttall, C.; Day, P.; *Chem. Mater.* **1998**, *10*, 3050.

(10) (a) Bellitto, C.; Day, P. *J. Mater. Chem.* **1992**, *2*, 265. (b) Stead, M. J.; Day, J. *Chem. Soc., Dalton Trans.* **1982**, 1081. (c) Fair, M. J.; Gregson, A. K.; Day, P.; Hutchings, M. T. *Physica B* **1977**, *86–88*, 657. (d) De Jongh, L. J. A.; Batterman, C.; Bose, F. R.; Miedema, A. R. *J. Appl. Phys.* **1969**, *40*, 1363. (d) Miedema, A. R.; van Kempen, H.; Huiskamp, W. J. *Physica* **1963**, *29*, 1266. (e) Yamada, I. *J. Phys. Soc. Jpn.* **1970**, *28*, 1585. (f) Velu, E.; Renard, J.-P.; Lecuyer, B. *Phys. Rev. B* **1976**, *14*, 5088.

(11) Clement, R.; Lacroix, P.; Evans, J. S. O.; O'Hare, D. *Adv. Mater.* **1994**, *6*, 794.

(12) (a) Wiegers, G. A.; Meerschaut, A. *Mater. Sci. Forum* **1992**, *100–101*, 101. (b) Suzuki, K.; Nakamura, O. *Mol. Cryst. Liq. Cryst.* **1998**, *311*, 143.

(13) (a) Goodenough, J. B. *Prog. Solid State Chem.* **1972**, *5*, 145. (b) Rao, C. N. R.; Cheetham, A. K. *Adv. Mater.* **1997**, *9*, 1009. (c) Salvador, P. A.; Doan, T.-D.; Mercey, B.; Raveau, B. *Chem. Mater.* **1998**, *10*, 2592.

(14) (a) Kurmoo, M.; Day, P.; Derory, A.; Estournès, C.; Poinot, R.; Stead, M. J.; Kepert, C. J. *J. Solid State Chem.* **1999**, *145*, 452. (b) Kurmoo, M. *Proc. R. Soc. A* **1999**, in press. (c) Kurmoo, M. *J. Mater. Chem.* **1999**, *9*, 2595.

(15) Wells, A. F. *Structural inorganic chemistry*; Oxford University Press: Oxford, 1984.

(16) Binder, K.; Young, A. P. *Rev. Mod. Phys.* **1986**, *58*, 801.

(17) De Jongh, L. J., Ed. *Magnetic Properties of Layered Transition Metal Compounds*; Kluwer Academic Publishers: Dordrecht, Boston, MA, 1990.

(18) (a) Kurmoo, M.; Graham, A. W.; Day, P.; Coles, S. J.; Hursthouse, M. B.; Caulfield, J. L.; Singleton, J.; Pratt, F. L.; Hayes, W.; Ducasse, L.; Guionneau, P. *J. Am. Chem. Soc.* **1995**, *117*, 12209. (b) Nicoud, J.-F. *Science* **1994**, *63*, 636.

(19) Heinrich, B.; Bland, J. A. C., Eds. *Ultrathin magnetic structures*; Springer-Verlag: Berlin, 1994.

(20) (a) Andrá, W.; Danan, H.; Mattheis, R. *Phys. Status Solidi* **1991**, *125*, 9. (b) Honda, Y.; Hirayama, Y.; Futamoto, M. *IEEE Trans. Magn.* **1998**, *34*, 1633.

Experimental Section

Synthesis. Chemicals were obtained from Fluka and Aldrich and used as obtained. All the compounds were prepared by the following procedure: $\text{Co}(\text{H}_2\text{O})_2(\text{NO}_3)_2$ (3 g) and either the acid or the sodium salt of the acid (1 g) were dissolved in 200 mL of a 1:1 mixture of distilled water and absolute ethanol and warmed to 40 °C. To this solution was added 3 mL of ammonium hydroxide (30%) dropwise to a pH of ~ 8 and stirred for 30–60 min. A dark blue to green precipitate is formed which was collected by filtration, washed with water, ethanol, and acetone, and dried in air. $\text{Co}_5(\text{OH})_8(\text{N}(\text{CN})_2)_2 \cdot 6\text{H}_2\text{O}$ was also prepared by the reaction of a suspension of $\text{Co}_2(\text{OH})_3(\text{NO}_3)$ in water with sodium dicyanamide at 25 °C for 24 h.

All the compounds were authenticated by chemical analyses for C, H, and N and thermogravimetric analyses were made to obtain the solvent content and mass percent of cobalt. Typical chemical analyses are as follows: found (calculated) % for $\text{Co}_5(\text{OH})_8(\text{C}_7\text{H}_{15}\text{CO}_2)_2 \cdot 4\text{H}_2\text{O}$, C 24.4 (24.35), H 5.87 (5.87), N 0.04 (0.00), Co 36.5 (37.44); for $\text{Co}_5(\text{OH})_8(\text{O}_2\text{CC}_6\text{H}_{12}\text{CO}_2) \cdot 5\text{H}_2\text{O}$, C 14.0 (13.87), H 4.28 (4.36), N 0.15 (0.00), Co 41.3 (42.52); for $\text{Co}_5(\text{OH})_8(\text{C}_{12}\text{H}_{25}\text{SO}_4)_2 \cdot (3\text{H}_2\text{O} \cdot 2\text{NH}_3)$, C 27.10 (27.46), H 6.63 (6.72), N 2.97 (2.67), Co 28.1 (27.2 calculated on the basis of CoO as the final product); and for $\text{Co}_5(\text{OH})_8(\text{C}_2\text{N}_3)_2 \cdot 6\text{H}_2\text{O}$, C 7.25 (7.16), H 2.30 (3.00), N 12.40 (12.53), Co 44.79 (43.92).

Physical Measurements. X-ray powder diffraction data were collected on a SIEMENS D-500 diffractometer equipped with monochromated $\text{Co K}\alpha 1$ radiation (1.789 Å). The data were collected in the 2θ range of 2–75° at an interval of 0.02° from samples which were dispersed in ethanol and allowed to set on a glass plate. Electron microscopy was performed on a TOPCON 002B microscope operating at 200 kV. Samples were placed on a copper grid with a holed polymer coating. Thermogravimetric analyses were performed in air on a SETARAM TGA system. Samples were placed in platinum containers and data were taken on heating at a rate of 6 °C per minute. All data were corrected for the empty container. Infrared data were recorded by transmission using a MATTSON FTIR spectrometer. Samples were prepared by dispersing the compounds in ethanol and allowing a drop of the suspension to evaporate onto a KBr plate. UV–vis spectra were recorded by transmission through a thin film of the compound dispersed in paraffin oil and held between two quartz plates on a Hitachi U-3000 spectrometer. A piece of white tissue paper soaked with the oil is used to compensate for the scattering of the powdered samples. XANES were recorded at 80 K at the Laboratoire pour l'Utilisation du Rayonnement Electromagnétique (LURE) in Orsay. The energy scale was calibrated by a Co foil. Temperature (4–300 K)-dependent magnetization measurements were made on a pendulum magnetometer in fields up to 1.3 T. Isothermal field-dependent magnetization data were collected on a Princeton Applied Research vibrating sample magnetometer (operating in field up to ± 1.6 T) and a Quantum Design SQUID MPMS-XL (ac and dc modes and maximum static field of ± 5 T). The latter was also used to collect magnetization data in the small applied field of ~ 1 Oe and in ac field of 1 Oe oscillating at 20 Hz. Further details on sampling techniques can be found in ref 6.

Results and Discussion

Syntheses. The reaction of cobalt nitrate with a base in the presence of a range of anions results in layered compounds. For example, with the nitrate ion three compounds, $\text{Co}(\text{OH})\text{NO}_3 \cdot \text{H}_2\text{O}$, $\text{Co}_2(\text{OH})_3\text{NO}_3$, and $\text{Co}_7(\text{OH})_{12}(\text{NO}_3)_2 \cdot 3\text{H}_2\text{O}$, have previously been isolated;^{21,22} the first two are pink and exhibit antiferromagnetic ordering and metamagnetism while the latter is green

and is described as a ferromagnet.²³ We have recently synthesized another derivative by using excess sodium nitrate in the reaction of cobalt nitrate with ammonia and characterized it as $\text{Co}_5(\text{OH})_8(\text{H}_2\text{O})_2(\text{NO}_3)_2$; it behaves as a ferrimagnet.^{14b} The advantage of using ammonium hydroxide instead of sodium or potassium hydroxide is the mildness of the former and the isolation of high purity compounds.²⁴ The addition of ethanol to the reaction serves two purposes: (a) to dissolve the acids and (b) for preventing the formation of trivalent cobalt by being slightly reducing. In addition, the products are fine particles which have the advantage of enhancing the magnitude of the observed coercive field^{6b} (see below) but is disadvantageous for crystallographic study. It is worth noting that the reaction of solid $\text{Co}_2(\text{OH})_3(\text{NO}_3)$ with sodium dicyanamide in water produces the same compound, $\text{Co}_5(\text{OH})_8(\text{N}(\text{CN})_2)_2 \cdot 6\text{H}_2\text{O}$, as that obtained by the reaction of ammonia with cobalt nitrate in the presence of sodium dicyanamide. It is also obtained by the reaction of a suspension of $\text{Co}^{\text{II}}(\text{N}(\text{CN})_2)_2$ in water with ammonia. Contrary to what has been described on several occasions,²⁵ the latter two observations suggest that the reaction of an alkyl carboxylate or sulfate with $\text{Co}_2(\text{OH})_3(\text{NO}_3)$ cannot be considered as “intercalation” or “anion exchange”. Reason being that the host is modified during the reaction.

X-ray Powder Diffraction and Structure. The XRD patterns for the four compounds are shown in Figure 1. The patterns are dominated by a principal progression of the 00/ Bragg reflections corresponding to the basal spacing which is characteristic of layered structures and two asymmetric broad in plane reflections at $d = 2.69$ and 1.55 Å. In some cases, there is an extra reflection at $d = 6.25$ Å which may correspond to one in-plane crystallographic axis and is twice the M–M distance of the triangular Brucite-like layer. The basal spacing (d_{001}) increases with the length of the anion in the following order, dicyanamide 11.5 Å, suberate 16.2 Å, caprylate 22.8 Å, and dodecyl sulfate 25.0 Å. We note that the difference in spacing for the carboxylate and the dicarboxylate, having the same number of carbon atoms in the chain, is 6.6 Å, implying that the dicarboxylate bridges adjacent layers.^{14b} It is also worth noting that the space between the layers are more efficiently packed for the carboxylate derivative than for the dicarboxylate. However, the lack of more X-ray diffraction information limits a thorough structural analysis.

Electron Microscopy. The powders of the compounds appear as irregular plates of maximum dimension of ~ 1 μm under the electron microscope. A typical electron diffraction pattern of a microcrystal of Co_5 -

(23) Laget, V.; Rouba, S.; Rabu, P.; Hornick, C.; Drillon, M. *J. Magn. Magn. Mater.* **1996**, 154, L7.

(24) (a) Mitchell, I. V., Ed. *Pillared Layered Structures; Current Trends and Applications*; Elsevier: London, 1990. (b) Leith, R. M. A. *Preparation and Crystal Growth of Materials with Layered Structure*; D. Reidel Publisher: Dordrecht, 1977.

(25) (a) Drillon, M.; Hornick, C.; Laget, V.; Rabu, P.; Romero, F. M.; Rouba, S.; Ulrich, G.; Ziessel, R. *Mol. Cryst. Liq. Cryst.* **1995**, 273, 125. (b) Laget, V.; Rabu, P.; Hornick, C.; Romero, F.; Ziessel, R.; Turek, P.; Drillon, M. *Mol. Cryst. Liq. Cryst.* **1997**, 305, 291. (c) Laget, V.; Drillon, M.; Hornick, C.; Rabu, P.; Romero, F.; Turek, P.; Ziessel, R. *J. Alloys Compd.* **1997**, 262, 423. (d) Laget, V.; Hornick, C.; Rabu, P.; Drillon, M.; Ziessel, R. *Coord. Chem. Rev.* **1998**, 178–180, 1533 and references therein. (e) Laget, V.; Hornick, C.; Rabu, P.; Drillon, M.; Turek, P.; Ziessel, R. *Adv. Mater.* **1998**, 10, 1024.

(21) Rouba, S. Thèse doctorat, Université Louis Pasteur, Strasbourg, France, 1996.

(22) Markov, L.; Petrov, K.; Petrov, V. *Thermochim. Acta* **1986**, 106, 283.

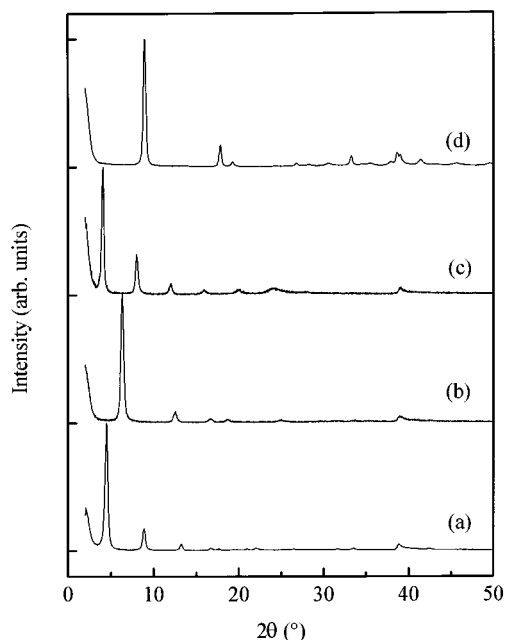


Figure 1. Powder X-ray diffraction patterns for (a) $\text{Co}_5(\text{OH})_8(\text{C}_7\text{H}_{15}\text{CO}_2)_2 \cdot 4\text{H}_2\text{O}$, (b) $\text{Co}_5(\text{OH})_8(\text{O}_2\text{CC}_6\text{H}_{12}\text{CO}_2) \cdot 5\text{H}_2\text{O}$, (c) $\text{Co}_5(\text{OH})_8(\text{C}_{12}\text{H}_{25}\text{SO}_4)_2 \cdot (3\text{H}_2\text{O} \cdot 2\text{NH}_3)$ and (d) $\text{Co}_5(\text{OH})_8(\text{C}_2\text{N}_3)_2 \cdot 6\text{H}_2\text{O}$ (Co $\text{K}\alpha 1$, $\lambda = 1.789 \text{ \AA}$).

$(\text{OH})_8(\text{C}_2\text{N}_3)_2 \cdot 6\text{H}_2\text{O}$ is shown in Figure 2a. There are two rings on which the most intense Bragg reflections are superposed. Within each ring there are six main reflections and two to four sets of six equidistant diffuse weak reflections. Furthermore, there appears to be four intense and two slightly less intense spots for each set. The estimated spacing of the inner and outer rings are 2.7 and 1.6 \AA , respectively; in good agreement with those observed in the XRD data. If we adopt the $\text{Zn}_5(\text{OH})_8(\text{H}_2\text{O})_2(\text{NO}_3)_2$ structure²⁶ and simulate the pattern (Figure 2b) expected if the crystal was aligned with the a axis (stacking axis) parallel to the incident radiation, we find that four of the six largest peaks within the inner ring correspond to the 021 set and the other two to the 002 set. Similarly, those of the outer ring correspond to the 023 and 040 sets, respectively. The weak diffused reflections outside the outer ring correspond to the 042 and 004 sets. The distribution of intensities is also in good agreement; for example, for the $C2/m$ space group the 001 is weaker than the 002 by a factor of 10. We should point out that the difference in d for the 002 and 021 in the inner ring or 023 and 040 in the outer ring is small and cannot be differentiated by the naked eye.

A similar analysis for the hexagonal system, $\text{Zn}_5(\text{OH})_8\text{Cl}_2 \cdot \text{H}_2\text{O}$,²⁷ shows that the inner ring is expected at 3.2 \AA and all six reflections are of equal intensity. The outer ring is at nearly the same distance (1.59 \AA) as for the monoclinic cell (1.56 \AA). The second major difference is in the position of the reflections in the outer ring relative to those in the first. In the hexagonal cell the reflections of both rings lie on the same radials while in the monoclinic cell those of the outer ring are offset with respect to those of the inner ring.

(26) (a) Stählin, W.; Oswald, H. R. *Acta Crystallogr. B* **1970**, *26*, 860. (b) Benard, P.; Auffredic, J. P.; Louer, D. *Thermochem. Acta* **1994**, *232*, 65.

(27) Allmann, R.; *Z. Kristallogr.* **1968**, *126*, 417.

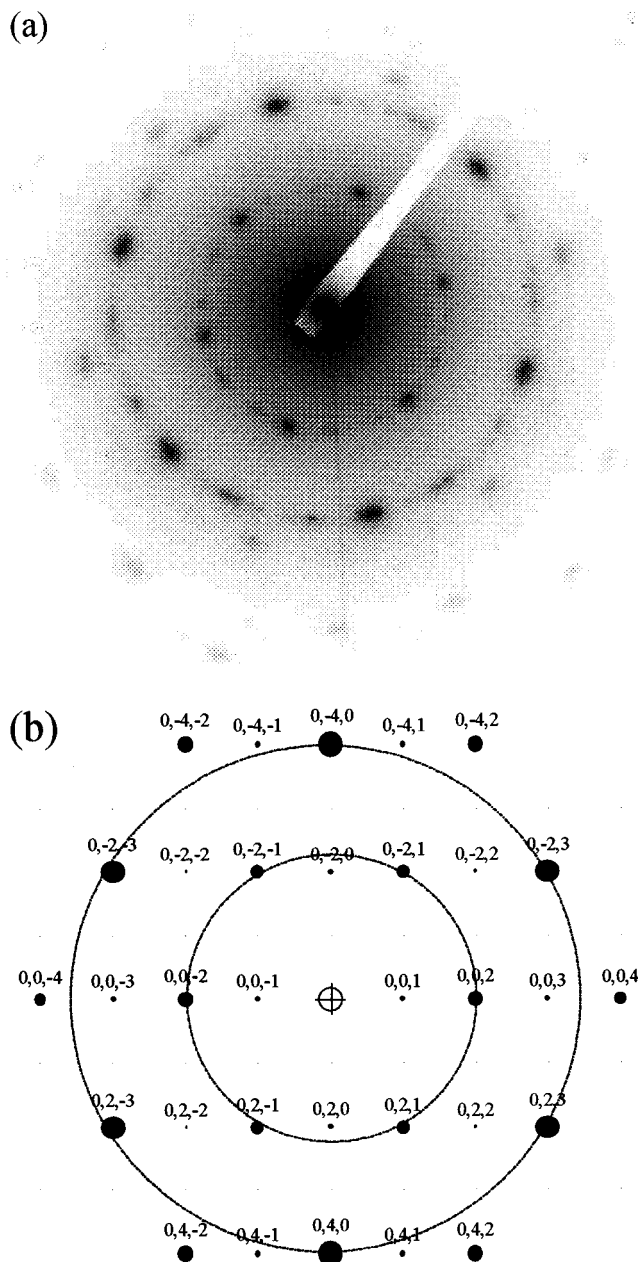


Figure 2. (a) Electron diffraction pattern of a plate crystal of $\text{Co}_5(\text{OH})_8(\text{C}_2\text{N}_3)_2 \cdot 6\text{H}_2\text{O}$ for a zone axis along a and (b) the simulated pattern using the atomic coordinates and cell parameters of $\text{Zn}_5(\text{OH})_8(\text{H}_2\text{O})_2(\text{NO}_3)_2$; the thin lines are guides to the eye.

Therefore, all evidence points in favor of a monoclinic cell. However, the presence of some fraction of the sample having a hexagonal unit cell cannot be excluded. This is suggested by the magnetic data detailed further on.

The structures of hexagonal $\text{Zn}_5(\text{OH})_8\text{Cl}_2 \cdot \text{H}_2\text{O}$ and monoclinic $\text{Zn}_5(\text{OH})_8(\text{H}_2\text{O})_2(\text{NO}_3)_2$ are shown in Figure 3.^{26,27} They consist of layers of $\text{Zn}_3(\text{OH})_8$ with octahedral Zn where one in four of the Zn in the Brucite-like layer is replaced by two tetrahedral Zn above and below each vacant position. Idealized structures of $\text{Co}_5(\text{OH})_8(\text{C}_7\text{H}_{15}\text{CO}_2)_2 \cdot 4\text{H}_2\text{O}$ and $\text{Co}_5(\text{OH})_8(\text{O}_2\text{CC}_6\text{H}_{12}\text{CO}_2) \cdot 5\text{H}_2\text{O}$ based on the triple-deck layer structure found for $\text{Zn}_5(\text{OH})_8(\text{H}_2\text{O})_2(\text{NO}_3)_2$ are shown in Figure 4 for layers "interdigitated" by the caprylate anions and for layers pillared by suberate anions. It is worth noting here that these

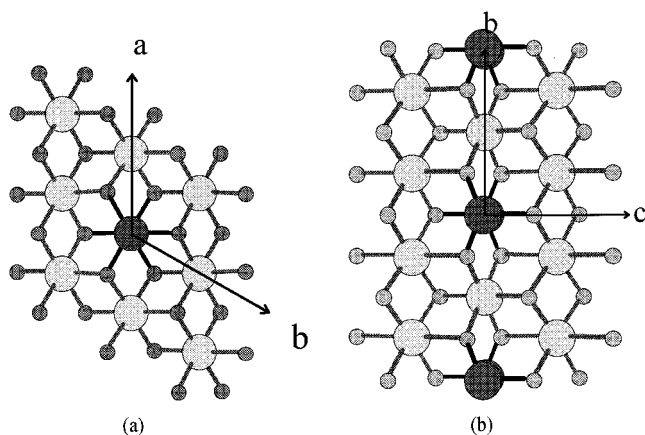


Figure 3. View of the layered structures of (a) hexagonal $\text{Zn}_5(\text{OH})_8\text{Cl}_2\cdot\text{H}_2\text{O}$ and of (b) monoclinic $\text{Zn}_5(\text{OH})_8(\text{H}_2\text{O})_2(\text{NO}_3)_2$ showing octahedral zinc (gray) and tetrahedral zinc (dark). Atomic coordinates taken from refs 26 and 27.

particular structures are found for Co and Zn and not for Cu or Ni which consist of only octahedral metal coordination and therefore single-deck layers.^{14a} From a chemical point of view the behavior of cobalt is more complex because (a) energetically both octahedral and tetrahedral coordination are possible, (b) oxidation of octahedral divalent cobalt to the trivalent state is facile, and (c) divalent and trivalent cobalt ions are equally stable. Previously, it was proposed that $\text{Co}_2(\text{OH})_3(\text{C}_{12}\text{H}_{25}\text{SO}_4)\cdot 2\text{H}_2\text{O}$ ²³ and the $\text{Co}_7(\text{OH})_{12}(\text{alkyl sulfate})_2\cdot x\text{H}_2\text{O}$ series,²⁵ prepared by anion exchange with $\text{Co}_2(\text{OH})_3(\text{NO}_3)$, adopt a single-deck structure containing both tetrahedral and octahedral metal centers. Similar suggestions were made for $\text{Co}_2(\text{OH})_{3.5}(\text{IMB})_{0.5}\cdot 2\text{H}_2\text{O}$, where IMB is the organic radical imino nitroxide benzoate.²⁵

Thermogravimetric Analysis. The thermogravimetric analyses in air are characterized by three weight losses: (a) at $110 \pm 20^\circ\text{C}$ which is endothermic and accounts for the loss of water or ammonia, (b) at $240 \pm 20^\circ\text{C}$ which is exothermic associated with the pyrolysis of the organic chain to form Co_3O_4 , and (c) at 950°C which is endothermic for the decomposition of Co_3O_4 to

CoO. The data for the sulfate is more complex due to the formation of sulfide and oxy-sulfide.

Infrared and UV-Vis Spectroscopies. The infrared spectrum is characterized by a broad band centered at 3450 cm^{-1} , characteristic of the OH stretching vibration. Three C-H modes are observed at 2955, 2920, and 2855 cm^{-1} . The carboxylate asymmetric and symmetric vibrations are observed at 1540 and 1400 cm^{-1} ; the difference in energy between the two bands is as expected for unidentate carboxylates.²⁸ The observation of only one of each for the dicarboxylate compounds suggests the two terminal carboxylate groups are equivalent. The sulfate bands are observed at 1214, 1061, and 983 cm^{-1} . Three C-N stretching modes of the dicyanamide ion are observed at 2271, 2249, and 2211 cm^{-1} and one bending mode at 1315 cm^{-1} ; in agreement with a single coordination of the dicyanamide through one of its nitrile nitrogen atom as found for *trans*-Ni(en)₂-N(CN)₂.^{6b}

The UV-vis absorption spectra of the four compounds, shown in Figure 5, are dominated by the d-d electronic transitions of the cobalt ion. In each case the spectrum is characterized by three bands, a pair at 15 650 and $16\,850\text{ cm}^{-1}$ and one at $20\,200\text{ cm}^{-1}$ which are respectively assigned to the ${}^4\text{T}_1(\text{P}) \leftarrow {}^4\text{A}_2$ of the tetrahedral cobalt which is split by spin-orbit coupling and to ${}^4\text{A}_{2g}(\text{P}) \leftarrow {}^4\text{T}_{1g}(\text{F})$ and ${}^4\text{T}_{1g}(\text{P}) \leftarrow {}^4\text{T}_{1g}(\text{F})$ of the octahedral cobalt.²⁹ We should point out that the spectra do not show any bands originating from Co^{III} which is expected to exhibit two bands in the visible region at $29\,200$ (${}^1\text{T}_{1g} \leftarrow {}^1\text{A}_{1g}$) and $20\,300\text{ cm}^{-1}$ (${}^1\text{T}_{2g} \leftarrow {}^1\text{A}_{1g}$) for low-spin Co^{III} of O_h parentage.

X-ray Absorption Spectroscopy. The cobalt K-edge XAS spectra of $\text{Co}_5(\text{OH})_8(\text{C}_7\text{H}_{15}\text{CO}_2)_2\cdot 4\text{H}_2\text{O}$, $\text{Co}_5(\text{OH})_8(\text{C}_2\text{N}_3)_2\cdot 6\text{H}_2\text{O}$, and of the reference Co^{II} compound, $\text{Co}_2(\text{OH})_3(\text{NO}_3)$, are shown in Figure 6. The preedge feature, originating from the $3d \leftarrow 1s$ transition, is observed at 7702 eV. The K-edge is characterized by one peak at 7719 eV for $\text{Co}_2(\text{OH})_3(\text{NO}_3)$ and by two overlapping peaks at 7715 and 7719 eV for $\text{Co}_5(\text{OH})_8(\text{C}_7\text{H}_{15}\text{CO}_2)_2\cdot 4\text{H}_2\text{O}$ and $\text{Co}_5(\text{OH})_8(\text{C}_2\text{N}_3)_2\cdot 6\text{H}_2\text{O}$. The additional peak at 7715 eV may originate from tetrahedral coordinated

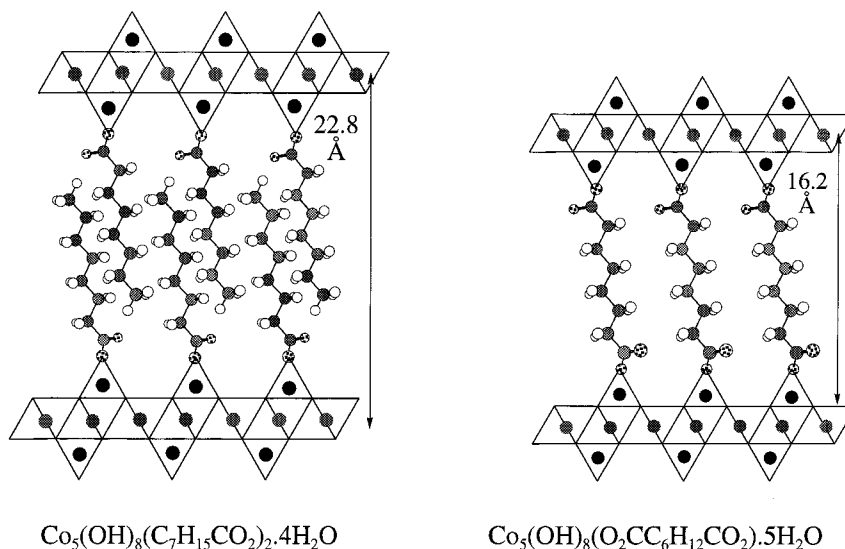


Figure 4. Idealized structures for $\text{Co}_5(\text{OH})_8(\text{C}_7\text{H}_{15}\text{CO}_2)_2\cdot 4\text{H}_2\text{O}$ and $\text{Co}_5(\text{OH})_8(\text{O}_2\text{CC}_6\text{H}_{12}\text{CO}_2)\cdot 5\text{H}_2\text{O}$ based on the triple-deck layer structure found for $\text{Zn}_5(\text{OH})_8(\text{H}_2\text{O})_2(\text{NO}_3)_2$ (data taken from ref 26).

Table 1. Summary of Magnetic Data

compound	d_{001} (Å)	C (cm ³ K/mol)	θ (K)	T_C (K)	$H_{coercive}$ (Oe) ^a	M_{sat} (μ_B) ^a	M_{rem} (μ_B) ^a
Co ₅ (OH) ₈ (C ₇ H ₁₅ CO ₂) ₂ ·4H ₂ O ^b	22.82	12.89	−60	57	8 300	2.30	1.22
Co ₅ (OH) ₈ (O ₂ CC ₆ H ₁₂ CO ₂) ₂ ·5H ₂ O ^b	16.21	13.47	−59	55	6 700	2.30	1.00
Co ₅ (OH) ₈ (C ₁₂ H ₂₅ SO ₄) ₂ ·(3H ₂ O·2NH ₃) ^b	24.97	12.23	−32	40	10 200	2.46	1.45
Co ₅ (OH) ₈ (C ₁₂ H ₂₅ SO ₃) ₂ ·5H ₂ O ^c	24.91	12.97	−36	50 ^d	19 000	2.72	1.44
Co ₅ (OH) ₈ (C ₂ N ₃) ₂ ·6H ₂ O ^b	11.56	13.45	−58	58	12 600	2.72	1.35

^a Value at 2 K. ^b This work. ^c Reference 14. ^d Estimated from the dc magnetization data in 200 Oe.

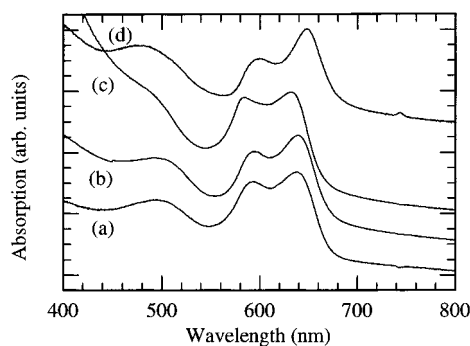


Figure 5. Visible absorption spectra of (a) Co₅(OH)₈(C₇H₁₅CO₂)₂·4H₂O, (b) Co₅(OH)₈(O₂CC₆H₁₂CO₂)₂·5H₂O, (c) Co₅(OH)₈(C₁₂H₂₅SO₄)₂·(3H₂O·2NH₃), and (d) Co₅(OH)₈(C₂N₃)₂·6H₂O.

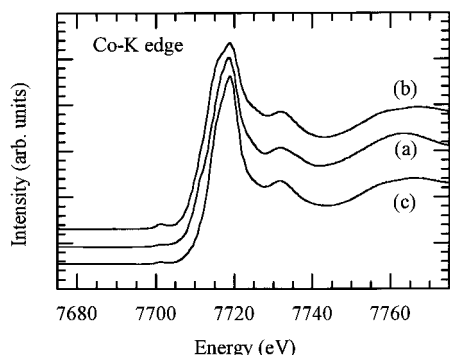


Figure 6. X-ray absorption spectra of the cobalt K-edge of (a) Co₂(OH)₃(NO₃), (b) Co₅(OH)₈(C₇H₁₅CO₂)₂·4H₂O, and (c) Co₅(OH)₈(C₂N₃)₂·6H₂O.

Co^{II}. The preedge peak is slightly more intense for Co₅(OH)₈(C₇H₁₅CO₂)₂·4H₂O and Co₅(OH)₈(C₂N₃)₂·6H₂O than for Co₂(OH)₃(NO₃), suggesting the lack of inversion symmetry on some sites for the former two compounds, in agreement with the presence of tetrahedral sites in the proposed structure.³⁰ The lack of any peak at higher energy, expected at 7722 eV for Co^{III}, excludes the presence of trivalent cobalt. This is in agreement with the proposal of Kamath et al.³¹ but not with that of Zeng et al.³²

Magnetic Properties. A summary of the magnetic data for the four compounds is given in Table 1. The temperature dependence of the moment represented by the product of susceptibility and temperature and of the

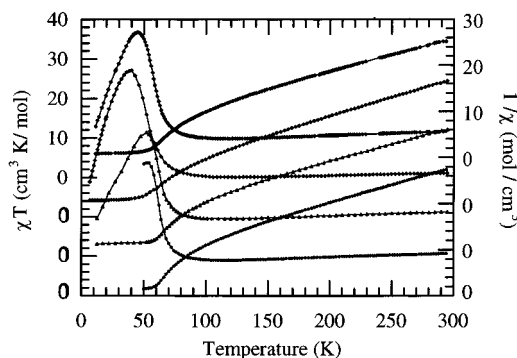


Figure 7. Temperature dependence of the inverse susceptibilities (right axis) and of the products of susceptibility and temperature (left axis) measured in applied field of ~12 000 Oe for (a) Co₅(OH)₈(C₇H₁₅CO₂)₂·4H₂O (open circles), (b) Co₅(OH)₈(O₂CC₆H₁₂CO₂)₂·5H₂O (open triangles), (c) Co₅(OH)₈(C₁₂H₂₅SO₄)₂·(3H₂O·2NH₃) (filled diamonds), and (d) Co₅(OH)₈(C₂N₃)₂·6H₂O (open diamonds). Note that the data are offset by 10 units for both the right and left axes.

inverse susceptibility are shown in Figure 7. All the compounds behave in a similar manner; their moment decreases to a minimum at ~120 K as the temperature is lowered from room temperature, followed by a continuous rise to a maximum at ~50 K. Below 50 K, the magnetization is saturated (vide supra). This behavior is typical for ferrimagnetic materials. We should note that it is also possible to observe this behavior for compounds containing octahedral Co^{II} because Co^{II} ($s = 3/2$) has a ground-state Kramers doublet and due to strong spin–orbit coupling the low-temperature state is considered to have an effective $s' = 1/2$.³³ The data showing a linear dependence of the inverse susceptibility with temperature (150–300 K) were analyzed by fitting to the Curie–Weiss law (Table 1). We observe that all the Weiss temperatures are negative suggesting short-range antiferromagnetic exchange. The fitted Curie constants are in good agreement with the statistical average of octahedral and tetrahedral Co^{II} ions.³⁴

The ac and dc magnetization were measured in near zero applied field (1 Oe) in the ordered state and around the critical temperature region. In each case, the data were collected on cooling. The results are shown in Figure 8. Spontaneous magnetization is observed by a sharp increase of dc magnetization and by a peak in both the in-phase and out-of-phase components of the ac magnetization. For the caprylate and suberate compounds there are an additional increase of the dc magnetization at ~30 K, which is accompanied by a

(28) Nakamoto, K. *Infrared and Raman spectra of inorganic and coordination compounds*; John Wiley: New York, 1986; p 230.

(29) Lever, A. P. B. *Inorganic Electronic Spectroscopy*; Elsevier: Amsterdam, 1986.

(30) Barrett, P. A.; Sankar, G.; Catlow, C. R. A.; Thomas, J. M. T. *J. Phys. Chem.* **1996**, *100*, 8977. (b) Moen, A.; Nicholson, D. G.; Rønning, M.; Lamble, G. M.; Lee, J.-F.; Emerich, H. *J. Chem. Soc., Faraday Trans.* **1997**, *93*, 4071. (c) Moen, A.; Nicholson, D. G.; Rønning, M.; Emerich, H. *J. Mater. Chem.* **1998**, *8*, 2533.

(31) Jayashree, R. S.; Kamath, P. V. *J. Mater. Chem.* **1999**, *9*, 961. (b) Kamath P. V.; Therese, G. H. A.; Gopalakrishnan, J. *J. Solid State Chem.* **1997**, *128*, 38.

(32) (a) Zeng, H. C.; Xu, Z. P.; Qian, M. *Chem. Mater.* **1998**, *10*, 2277. (b) Xu, Z. P.; Zeng, H. C. *Chem. Mater.* **1999**, *11*, 67.

(33) Griffiths, J. S. *The theory of transition-metal ions*; Cambridge University Press: Cambridge, 1964; p 332.

(34) Mabbs, F. E.; Machin, D. J. *Magnetism and Transition Metal Complexes*; Chapman and Hall: New York, 1973.

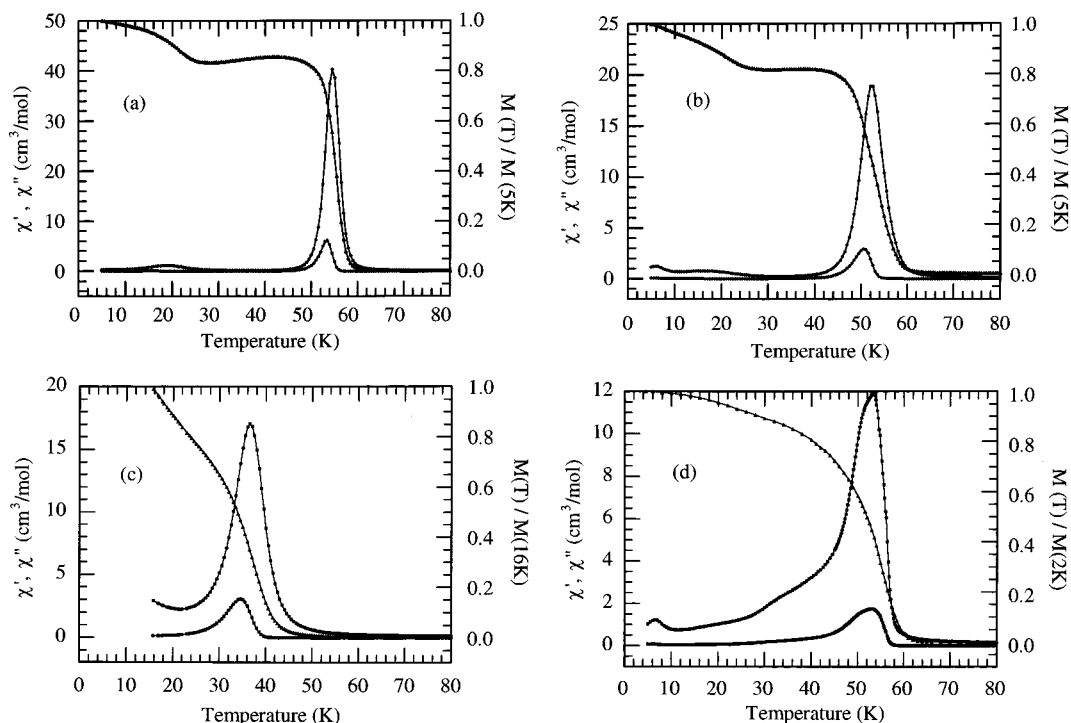


Figure 8. Temperature dependence of the dc magnetization in ~ 1 Oe and the in-phase and out-of-phase ac magnetization in an applied field of 1 Oe of (a) $\text{Co}_5(\text{OH})_8(\text{C}_7\text{H}_{15}\text{CO}_2)_2 \cdot 4\text{H}_2\text{O}$, (b) $\text{Co}_5(\text{OH})_8(\text{O}_2\text{CC}_6\text{H}_{12}\text{CO}_2) \cdot 5\text{H}_2\text{O}$, (c) $\text{Co}_5(\text{OH})_8(\text{C}_{12}\text{H}_{25}\text{SO}_4)_2 \cdot (3\text{H}_2\text{O} \cdot 2\text{NH}_3)$, and (d) $\text{Co}_5(\text{OH})_8(\text{C}_2\text{N}_3)_2 \cdot 6\text{H}_2\text{O}$.

weaker peak in the ac magnetization. This may be due to the presence of slight amount of another phase, e.g.: the hexagonal form. Comparing the dc and ac magnetization data of these two-dimensional compounds to those of three dimension it is not obvious what is the critical temperature.³⁵ For the 3D mean field magnets, $\text{M}^{\text{II}}(\text{N}(\text{CN})_2)_2$,⁶ spontaneous magnetic ordering is characterized by a discontinuous jump in the dc magnetization which coincide with the peak in the in-phase ac magnetization and to the nonzero out-of-phase ac magnetization. For the 2D compounds studied here, the onset of spontaneous magnetization is sluggish and the peak in the in-phase and the onset of the out-of-phase components of the ac magnetization do not coincide in temperature. In strict terms the critical temperature is defined at the point where the out-of-phase ac magnetization is none zero. Here, we have adopted this convention in defining the Curie temperature.

Isothermal magnetization have been measured at different temperatures between 2 and 100 K. Above the Curie temperature it is weakly field dependent and linear. Close to T_C the magnetization becomes nonlinear with an increasing curvature as the critical temperature is reached. Just below the transition hysteresis is observed; both the coercive field and the remanant magnetization increase as the temperature is lowered. The data for the lowest temperature studied are shown in Figure 9 and the maximum coercive field and remanant magnetization are listed in Table 1. We note that the magnetization is still increasing even in field

of 50 000 Oe, suggesting incomplete reversal of the moments.³⁶ This implies that the anisotropy field is large. The slanting shape and change of gradient of the hysteresis loop may originate from two possible effects: the large demagnetizing field due to the flat plate geometry of the particles and/or to the presence of a second phase. The wide hysteresis is due to the large magnetocrystalline anisotropy which is derived from the synergy of several factors: (a) large single-ion anisotropy for cobalt, (b) shape anisotropy, and (c) the alignment of the moment perpendicular to the layers.^{19,20,36} The situation is analogous to the large coercive fields observed for hexagonal ferrites compared to three-dimensional ferrites.³⁷ The values of the magnetization in the maximum field (5 T) attainable with our SQUID approach $3 \mu_B$. This value is consistent with the proposed structure comprising of two antiferromagnetically coupled sublattices within a layer; one consisting of cobalt in octahedral sites (3 per formula unit) and the other in tetrahedral sites (2 per formula unit). Thus the saturation magnetization in the ordered state per mole of a Co_5 compound is given by

$$M_{\text{sat}} = |3 \times g_{\text{oct}} \times \frac{3}{2} - 2 \times g_{\text{tet}} \times \frac{3}{2}| = 3N\mu_B$$

assuming $g_{\text{oct}} = g_{\text{tet}} = 2$.

It is worth doing some moment counting³⁸ for compounds of different stoichiometry to understand the type of magnetic ordering. For a ferromagnetic Co_2 compound which contains only octahedral sites, the magnetization

(35) (a) Domb, C. *The Critical Point*; Taylor Francis: London, 1996. (b) Stanley, H. E. *Introduction to Phase Transitions and Critical Phenomena*; Clarendon Press: Oxford, 1971. (c) Pokrovsky, V. L.; Uzmin, G. V. In *Magnetic Properties of Layered Transition Metal Compounds*; De Jongh, L. J., Ed.; Kluwer Academic Publishers: Dordrecht, Boston, MA, 1990.

(36) Chikazumi, S. *Physics of Magnetism*; John Wiley: New York, 1978.

(37) (a) Shirk, B. T.; Buessem, W. R. *J. Appl. Phys.* **1969**, *40*, 1017. (b) Bayer, G. *J. Am. Ceram. Soc.* **1960**, *43*, 495.

(38) Herpin, A. *Theorie du Magnetisme*; Presse Universitaire de France: Paris, 1968.

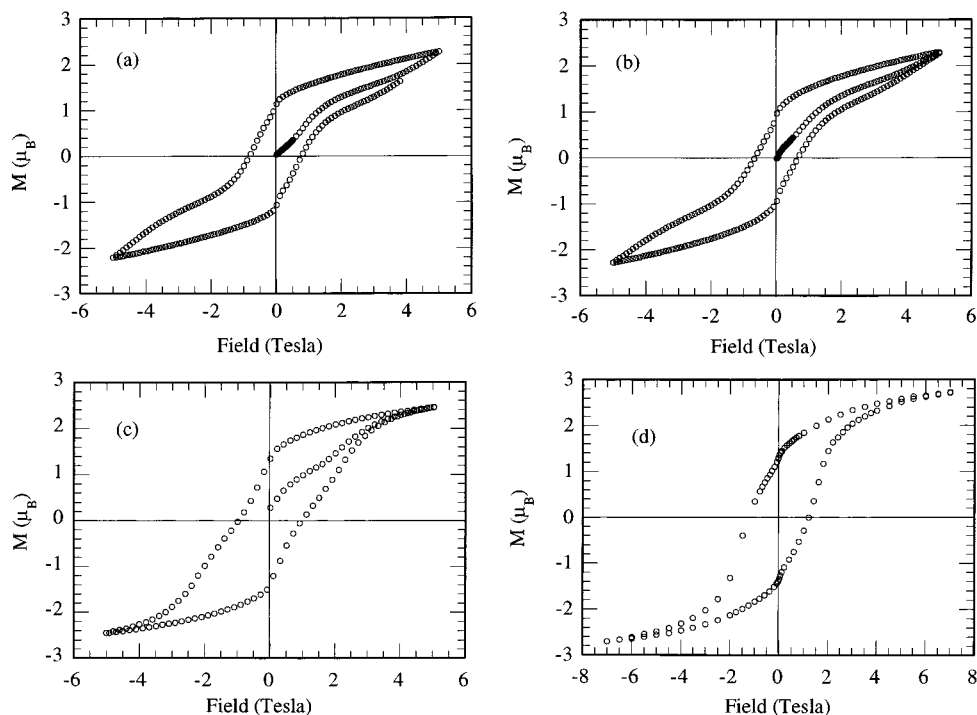


Figure 9. Field dependent magnetization at 2 K after zero field cooled of (a) $\text{Co}_5(\text{OH})_8(\text{C}_7\text{H}_{15}\text{CO}_2)_2 \cdot 4\text{H}_2\text{O}$, (b) $\text{Co}_5(\text{OH})_8(\text{O}_2\text{CC}_6\text{H}_{12}\text{CO}_2) \cdot 5\text{H}_2\text{O}$, (c) $\text{Co}_5(\text{OH})_8(\text{C}_{12}\text{H}_{25}\text{SO}_4)_2 \cdot (3\text{H}_2\text{O} \cdot 2\text{NH}_3)$, and (d) $\text{Co}_5(\text{OH})_8(\text{C}_2\text{N}_3)_2 \cdot 6\text{H}_2\text{O}$.

per mole is given by

$$M_{\text{sat}} = |2 \times g_{\text{oct}} \times \frac{3}{2}| = 6N\mu_B$$

while for an antiferromagnet, as for example $\text{Co}_2(\text{OH})_3(\text{NO}_3)$, the magnetization is linear with field as follows:

$$M = \chi_{\perp} H$$

where H is the applied field.

If there are two sublattices, one of tetrahedral and the other of octahedral coordination, as that proposed for $\text{Co}_2(\text{OH})_3(\text{C}_{12}\text{H}_{25}\text{SO}_4) \cdot 2\text{H}_2\text{O}$,²³ then the magnetization is given by

$$M = |1 \times g_{\text{tet}} \times \frac{3}{2} - 1 \times g_{\text{oct}} \times \frac{3}{2}| \sim 0N\mu_B$$

For a Co_7 compound, e.g., $\text{Co}_7(\text{OH})_{12}(\text{alkyl sulfate})_2 \cdot x\text{H}_2\text{O}$,²⁵ there are five octahedral Co^{II} and two tetrahedral Co^{II} per formula unit; assuming the two sublattices are the tetrahedral and octahedral sites as for the Co_5 compounds, the expected saturation magnetization is

$$M_{\text{sat}} = |(5 \times g_{\text{oct}} \times \frac{3}{2} - 2 \times g_{\text{tet}} \times \frac{3}{2})| = 9N\mu_B$$

Therefore, the saturation magnetization is a good guide of the stoichiometry and hence the structure.

The comparison made in the Introduction has shown that increasing the number of atoms in the bridging units dramatically decreases the Curie temperature. While in the series of layered compounds three-dimensional long-range magnetic ordering at temperatures as high as 58 K has been observed for bridges consisting of as many as 15 atoms and layers separated by as much as 29 Å. Through such long alkyl chains, the magnetic exchange interaction between cobalt on adjacent layers is expected to be negligible and even if

the layers are covalently bridged the exchange interaction through bonds is expected to be small as it follows a R^{-10} dependence,³⁹ where R is the distance between the spin centers. On the other hand purely electrostatic dipolar interaction between the layers is proportional to R^{-3} , which becomes more important at large distance.⁴⁰ A dipolar mechanism can be effective at large distance if the moments are large. For the layered compounds, this is achieved by short-range magnetic interactions.⁴⁰ As the temperature is lowered the correlation length within the layer, which depends on the magnitude of the near-neighbor exchange, increases. The exponential increase of the ac and dc magnetization in small applied field (Figure 8) and the noncoincidence of the temperature of the peak in the in-phase ac and that of the out-of-phase component of the ac magnetization are indications of the increase of the correlation length as T_C is approached.³⁵ Considering the monoclinic structure proposed earlier (Figures 3 and 4), the number of exchange interactions may be broken down to the following: four $J_1(\text{Co}_{\text{oct}}\text{A} - \text{Co}_{\text{oct}}\text{B})$, one $J_1'(\text{Co}_{\text{oct}}\text{A} - \text{Co}_{\text{oct}}\text{A})$, two $J_2(\text{Co}_{\text{oct}}\text{A} - \text{Co}_{\text{tet}})$, and $J_2'(\text{Co}_{\text{oct}}\text{B} - \text{Co}_{\text{tet}})$ and for the hexagonal structure there are five $J_1(\text{Co}_{\text{oct}} - \text{Co}_{\text{oct}})$ and six $J_2(\text{Co}_{\text{oct}} - \text{Co}_{\text{tet}})$. From the observed data we expect J_1 to be ferromagnetic and J_2 to be antiferromagnetic and the dominant of the two is J_2 . Since the critical temperature of the transition depends on the most dominant exchange interaction within the layer, it is therefore different for the two possible crystal structures. The critical temperature is also expected to increase with the value of spin quantum number (s); a point which agree with the experimental observations for the nickel and cobalt compounds although they are of different structures. Within the dipolar mechanism

(39) Bloch, D. *J. Phys. Chem. Solids* **1966**, 27, 881.

(40) (a) Durrant, E. *Magnétostatique*; Masson et Cie: Paris, 1968.
(b) Drillon, M.; Panissod, P. *J. Magn. Magn. Mater.* **1998**, 188, 93.

the critical temperature is expected to be a very slowly varying function of the distance when R is large (> 10 Å). The observation for this set of compounds is in good agreement (Table 1). Most importantly, introducing an exchange pathway through alkyl or aryl dicarboxylate bridges between the layers has no discernible effect on the transition temperature.^{14b} This, therefore, confirms that dipolar interaction at these distances is more important than exchange interaction through bonds.^{14,41} The fact that we have ferromagnetically coupled layers is a good indication that the moments are perpendicular to the planes, which is expected for spin carriers having large spin-orbit coupling as evidenced by the magnitude of the coercive force observed. A similar observation of a large coercive field has recently been noted by Kahn et al.⁴² in studies on the hard molecule-based magnet [(Etrad)₂Co₂{Cu(opba)}₃]·S where Etrad⁺ = radical cation, opba = *o*-phenylenebis(oxamato), and S = DMSO_{1.5}H₂O_{0.25}. In general, the most energetically favorable configuration when the moments are in the plane of a Heisenberg system is antiferromagnetic stacking.^{3,17}

Conclusion

A series of layered cobalt hydroxides incorporating several anions has been synthesized and characterized by several techniques. Using a combination of powder

X-ray and electron diffraction their structures are proposed to comprise of layers of divalent cobalt in octahedral coordination sandwiched by two layers of cobalt in tetrahedral coordination separated by the anions in the galleries. Long-range magnetic ordering between the two uncompensated sublattices results in ferrimagnets with Curie temperatures of up to 58 K, a coercive field of 12 000 Oe, and a magnetization of $\sim 3 \mu_B$ at 2 K. The chemical or physical nature of the anions do not influence the magnetic properties and, therefore, adds support to the proposed dipolar mechanism for the long-range magnetic orderings. Although the unusual magnetic properties are explained by a simple qualitative model more quantitative theoretical analyses are required. Further work on the chemistry of these materials to increase the intralayer interactions is in progress, aiming at increasing the Curie temperature to room temperature while keeping the magnetic hardness.

Acknowledgment. This work was funded by the CNRS-France (contrat Matériaux) and the EEC (Molecular Magnetism: from Materials toward Devices; ERBFMRXCT 980181). I am grateful to N. Finck, R. Poinot, and A. Derory for technical assistance, Dr. C. Mathonière of Université de Bordeaux I for the ac susceptibility measurements of Co₅(OH)₈(C₂N₃)₂·6H₂O, Dr. M. Richard-Plouet (Strasbourg) for electron microscopy, and Dr. A. Travers for her help with XAS at LURE. I acknowledge many useful discussions with Dr. C. J. Kepert of University of Sydney.

CM991099F

(41) Cano, J.; De Munno, G.; Sanz, J. L.; Ruiz, J. L.; Faus, R.; Lloret, J. F.; Julve, M.; Caneschi, A. *J. Chem. Soc., Dalton Trans.* **1997**, 1915.

(42) Vaz, M. G. F.; Pinheiro, L. M. M.; Stumpf, H. O.; Alcântara, A. F. C.; Golhen, S.; Ouahab, L.; Cador, O.; Mathonière, C.; Kahn, O. *Chem. Eur. J.* **1999**, 5, 1486.